Analysis of Oscillatory Neural Activity in Series Network Models of Parkinson's Disease During Deep Brain Stimulation

Clare M. Davidson*, Annraoi M. de Paor, Hayriye Cagnan, and Madeleine M. Lowery

***Abstract*—Parkinson's disease is a progressive, neurodegenerative disorder, characterized by hallmark motor symptoms. It is associated with pathological, oscillatory neural activity in the basal ganglia. Deep brain stimulation (DBS) is often successfully used to treat medically refractive Parkinson's disease. However, the selection of stimulation parameters is based on qualitative assessment of the patient, which can result in a lengthy tuning period and a suboptimal choice of parameters. This study explores fourth-order, control theory-based models of oscillatory activity in the basal ganglia. Describing function analysis is applied to examine possible mechanisms for the generation of oscillations in interacting nuclei and to investigate the suppression of oscillations with high-frequency stimulation. The theoretical results for the suppression of the oscillatory activity obtained using both the fourth-order model, and a previously described second-order model, are optimized to fit clinically recorded local field potential data obtained from Parkinsonian patients with implanted DBS. Close agreement between the power of oscillations recorded for a range of stimulation amplitudes is observed ($R^2 = 0.69 - 0.99$). The results suggest that the behavior of the system and the suppression of pathological neural oscillations with DBS is well described by the macroscopic models presented. The results also demonstrate that in this instance, a second-order model is sufficient to model the clinical data, without the need for added complexity. Describing the system behavior with computationally efficient models could aid in the identification of optimal stimulation parameters for patients in a clinical environment.**

***Index Terms*—Basal ganglia, control theory, mean field model, Parkinson's disease, pathological oscillations.**

I. Introduction

OSCILLATORY rhythms form an integral part of the central nervous system, although their exact functional significance has not yet been determined [1], [2]. In relation to the motor function of cortical and subcortical areas of the brain, growing evidence suggests that oscillations in the beta frequency range (13–30 Hz), in addition to those in the gamma frequency range (31–100 Hz), are of particular importance. Cortical beta oscillations have been shown to display event-related desynchronization prior to the initiation of movement, suppression during movement, with a rebound event-related synchronization immediately afterward [2]. This pattern is also observed in the subcortical basal ganglia [1]. Cortical stimulation at 20 Hz, which lies within the beta frequency range, slows motor output, lending weight to the causal rather than epiphenomenological nature of these oscillations [3]. Koelewijn *et al.* found a stronger beta rebound occurring in response to movement errors compared to the normal rebound following the cessation of movement, which they propose reflects involvement in an active inhibition response [4].

The depletion of dopamine in Parkinson's disease enhances the rhythmic oscillatory activity compared with that present in the healthy cortico-basal ganglia-thalamocortical system [5]. It is hypothesized that the normal dopaminergic system supports the segregation of the functional subcircuits of the basal ganglia [6], with the depletion of dopamine in Parkinson's disease believed to cause a breakdown of this segregation, leading to abnormal synchrony of neuronal activity [7], [8]. Parkinson's disease is characterized by enhanced beta rhythmical activity in the subthalamic nucleus (STN), globus pallidus pars externa (GPe) and globus pallidus pars interna (GPi), with the cerebral cortex postulated as being a likely source of this exaggerated synchronized activity [1]. Functional MRI has revealed an increase in the functional connectivity in the cortico-basal ganglia-thalamocortical system in Parkinson's disease [9]. Although this could occur as a consequence of the changes in the activity of these circuits in the diseased state [10], the suggestion that the loss of striatal dopamine could cause the changes in connectivity to occur is supported by results presented in [11] where dynamic causal modeling was used to characterize and compare connections in the cortico-basal ganglia-thalamocortical circuit. The connections to and from the STN were found to strengthen and promote synchronous beta oscillations in the untreated compared to the treated Parkinsonian state [11]. In [12], simultaneous magnetoencephalography and local field potential (LFP) recordings in patients with Parkinson's disease revealed distinct coupling in the beta-band frequency between the motor cortex area and the STN providing further support of their frequency-dependent functional connectivity. Studies in animal models of Parkinson's disease also support the hypothesis that altered connectivity in the cortico-basal ganglia-thalamocortical circuit plays a key role in the pathology of the disease [13], [14].

Bradykinesia and rigidity, hallmark motor symptoms of Parkinson's disease, have been shown to correlate with

Manuscript received January 7, 2015; revised May 20, 2015 and July 17, 2015; accepted August 19, 2015. Date of publication August 19, 2015; date of current version December 17, 2015. This work was supported by the Science Foundation Ireland under Grant 10/RFP/ECE2720. This paper was presented in a preliminary form at the IEEE Engineering in Medicine and Biology Society Neural Engineering Conference, San Diego, CA, USA, 2013. *Asterisk indicates corresponding author.*

*C. M. Davidson is with the School of Electrical, Electronic and Communications Engineering, University College Dublin, Dublin, Ireland (e-mail: clare.davidson@ucd.ie).

A. M. de Paor and M. M. Lowery are with the School of Electrical, Electronic and Communications Engineering, University College Dublin.

H. Cagnan is with the University of Oxford.

Digital Object Identifier 10.1109/TBME.2015.2475166

synchronous beta-band oscillatory activity in the basal ganglia [15], [16]. A correlative relationship between limb tremor in patients and oscillatory activity in the theta (or tremor) frequency range has also been established [17]. Dopaminergic medication has been shown to decrease the synchronous beta activity and improve the motor symptoms of the disease [18], [19]. A recent study by Beudel *et al.* showed correlation between deep brain stimulation (DBS)-induced suppression in the power of oscillations in the low gamma frequency range (31–45 Hz) and the reduction in the amplitude of the resting tremor recorded in Parkinsonian patients [20]. DBS also acts to suppress the pathological oscillations in the beta frequency band, with a parallel improvement in the motor symptoms of Parkinson's disease observed [15], [21], although a direct causal link, as well as an exact mode of action, remains yet to be established. This evidence provides support for the use of the oscillatory beta-band activity as a biomarker of Parkinson's disease in order to guide the programming of DBS devices or to use in conjunction with closed-loop systems [22], [23].

Mathematical modeling provides a valuable pathway for testing new hypotheses and gaining a greater understanding of the cortico-basal ganglia network and DBS. Models of the cortico-basal ganglia network range from detailed cellular level models to reduced, neural mass-type models. A network model comprised of conductance-based biophysical models of each included cell type, the STN, GPe, GPi, and thalamus, introduced by [24], has been implemented and extended in a number of subsequent studies exploring the effect of DBS [25]–[27]. Cellular level models have also been utilized to explore the STN-GPe pacemaking hypotheses [28], [29]. Other detailed computational models that have been used to explore the effect of applied DBS have also been developed [30]–[32]. However, although examination of interactions occurring at the cellular level can yield valuable insight into possible pathological mechanisms at a local level, it seems that examining the behavior of the model at a system level should result in a deeper understanding of Parkinson's disease and DBS. In addition, modeling systems at the level of individual neurons can lead to a model becoming unwieldy and intractable. Hence, in many studies, a phenomenologically based model, often referred to as a "neural mass" or "lumped parameter" model, is designed, with simplifying assumptions made about the behavior at the cellular level. One of the earliest models representing the collective dynamics of neural populations comprising of distinct excitatory and inhibitory subpopulations was introduced by Wilson and Cowan in [33], and forms the basis for many of the more recent neural models. Mathematical models can also be designed to illustrate and explore a particular phenomenon occurring in a physiological system, without a foundation on the anatomy or physiology of the system [34].

In an attempt to gain a greater understanding of the Parkinsonian basal ganglia and the mechanism of action of DBS, a number of models based on this phenomenological idea have been developed. Holgado *et al.* demonstrated the intrinsic oscillatory capabilities of the STN-GPe network in a model based on anatomical and electrophysiological studies [35]. Rather than simulating the dynamics and firing times of individual neurons, their model represented changes in the firing rates of neural populations. A more comprehensive, neural mass model of the cortico-basal ganglia-thalamocortical circuit based on LFP data recorded from a rat model of Parkinson's disease was presented in [13]. In this study, under simulated dopamine depletion, the connection strength of cortical, hyperdirect input to STN was observed to increase, and the STN input to GPe decreased. Pathological, synchronized oscillations were modeled in a simplified manner and used to explore the effects of different types of desynchronizing brain stimulation techniques in number of publications from Tass *et al.* [36]–[38]. In a similar way, the models we present here aim to capture the key pathological mechanisms of Parkinson's disease, without including details of the cellular morphology of the system. This is to allow the models to be readily explored and analyzed, and track the complex system in a simplified manner, without reverse engineering, the failing basal ganglia [39].

In [40], a second-order macroscopic mathematical model used to represent oscillatory activity of a synchronous group of neurons was presented. The model was tuned to specifically capture key features of the physiological system representing a closed loop within the cortico-basal ganglia-thalamocortical system and to generate the pathological oscillations that occur here in Parkinson's disease. The suppression of these oscillations by the injection of high-frequency stimulation was examined, and the results compared to clinical data previously published in [41]. However, the model analyzed is the simplest that can generate oscillatory activity, and the analysis presented cannot readily be extended to higher order models. More complex, higher order models may more accurately represent the dynamics of the basal ganglia-thalamocortical system by modeling the interaction of two or more nuclei, allowing the parameters of each to be varied individually.

This study examines and analyzes two fourth-order models of oscillatory activity with the aim of capturing the dynamics of the system being considered while remaining analytically tractable. In developing the models, we consider the cortico-basal ganglia-thalamocortical system as a complex network of coupled nuclei, in which the level of synchronization and coupling between neurons within and across different nuclei increases as dopamine is depleted in Parkinson's disease. Within this network, under conditions of dopamine depletion, the enhanced coupling may lead the reciprocally connected STN-GPe loop to act as a central pacemaker, as discussed in [42], or alternatively, the entire network may experience a loss of segregation [17] reducing to a simpler, tightly coupled network of interacting oscillators. Each fourth-order model is based on a combination of two of the previously described second-order models. A series model with separate self-oscillating feedback loops, and a reduced fourth-order series model are both considered. The describing function is applied to analyze the models. Two describing functions are combined in a novel way, enabling the application of this established theory to the fourth-order models. The theoretical analysis presented is extendable to higher order models, providing a framework for the theoretical analysis of more complex networks modeled in this way, similar to that described in [43]. Possible mechanisms for the generation of pathological

oscillatory activity are explored by studying the interaction of the two distinct nuclei. The suppression of oscillations with the application of high-frequency stimulation representing DBS is examined in the fourth-order series (reduced) model. In order to examine whether the addition of a second nuclei improves the accuracy of the model, the theoretical results obtained for the fourth-order series (reduced) model, and the original second-order model, are compared to clinically recorded LFP data, and the fits obtained are compared. Both models are shown to be capable of capturing the dynamics of the beta-band LFP activity as the amplitude of the applied DBS is increased. The models presented in this study are designed with the aim of being readily analyzed such that their translation to a clinical environment as a tool to aid in the identification of optimal DBS parameters on a patient by patient basis would be possible.

II. Methods

Oscillatory activity in the basal ganglia can be recorded in the form of the LFP. LFPs reflect the summation of local, rhythmic, synchronized subthreshold activity in presynaptic terminals and postsynaptic neurons [7], [44]. The models presented in this study aim to capture the dynamics of the cortico-basal ganglia-thalamocortical system as they appear to an external observer, by reproducing the synchronized oscillatory activity recorded in the vicinity of the STN. Although comparisons are drawn between the models and the physiological system, each second-order nucleus, consisting of a nonlinear, sigmoidal arctan function in series with a second-order transfer function, essentially represents a reduced oscillating system. The individual, physiological components modeled by each nucleus are assumed to display synchronous dynamics. This system-level model of the neural population explored in this study follows concepts of neural mass modeling [45].

The fourth-order models each consist of two reciprocally connected second-order models, which are used to represent two distinct neural ensembles connected in series, Figs. 1 and 2. These could be chosen to represent any two individual interconnected nuclei. For example, each loop in Fig. 1 could represent a nucleus with self-excitation that would enable it to generate oscillations, or two coupled nuclei, which form a single oscillator, as is considered in [40]. The STN-GPe loop could be modeled as shown in Fig. 2. The choice of excitatory-inhibitory interconnections between the two nuclei reflects the physiological interconnections existing between both the cortex and basal ganglia, and the STN and GPe [46]. The theoretical analysis presented here, based on describing function analysis, can be extended to include as many individual groups of neurons as required. A complete description of the second-order model, and the associated analysis, is provided in an earlier paper [40].

Imaging and electrophysiological studies indicate that the depletion of dopamine in Parkinson's disease is associated with an increase in the functional connectivity within the basal ganglia, leading to abnormal, synchronous neural activity [9], [47]. Connectivity is modulated by the parameter h_n, which represents the effect of dopamine on the system; a decrease in h_n leads to an increase in the gain (or functional connectivity) of the system,

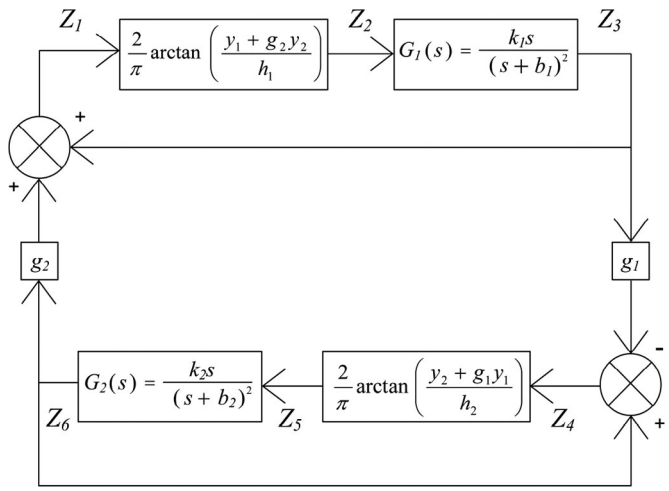

Fig. 1. Schematic diagram of the fourth-order series model (with feedback) representing neural synchrony in two interconnected second-order loops. The two networks are coupled through g_1 and g_2. For excitatory-excitatory coupling $(+/+)$ $g_1 = -g_2 > 0$. For excitatory-inhibitory $(+/-)$ coupling $g_1 = g_2$.

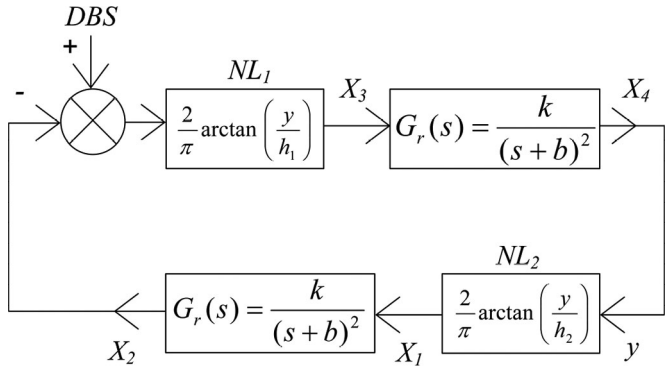

Fig. 2. Schematic diagram of the fourth-order model of neural synchrony comprised of a series connection of two second-order models of synchronous activity as presented in [40]. For notational simplicity, the nonlinear element in the first nuclei is labeled as NL_1 and in the second nuclei similarly termed NL_2. The DBS is applied additively at the input to NL_1.

resulting in an increase in the amplitude of the model output. Mathematically, as h_n decreases, the slope of the sigmoid, and thus, the responsiveness of the feedback loop, increases.

A. Fourth-Order Series Model (With Feedback)

In order to explore mechanisms by which oscillatory neural activity can be generated through the interaction of different frequencies, a fourth-order model of the basal ganglia-thalamocortical system is presented and analyzed using the describing function approach. Interaction between distinct loops, either tuned to oscillate at a particular frequency or inherently nonoscillating, can give rise to oscillations at other frequencies. The fourth-order series model (with feedback) presented in Fig. 1, consists of two second-order models of oscillatory activity coupled with two variable gain terms, g_1 and g_2. The coupling shown in Fig. 1 is an excitatory-inhibitory configuration. This reflects the physiological excitatory-inhibitory interconnections

that exist between either the STN-GPe, or the cortex-basal ganglia. Within the fourth-order series model (with feedback), each second-order model includes an individual feedback loop, and is capable of oscillatory activity when appropriately tuned. The parameters of the second-order models can be chosen such that they are nonoscillating, or initialized to oscillate at either the same or different frequencies, with the frequency of the resulting output from the model changing as a function of the gain in the loop, $g_1 g_2$. The interaction of two different initial frequencies is examined through simulation of the model with the interconnections in an excitatory-excitatory configuration. This was achieved by setting $g_1 = -g_2$.

To facilitate the theoretical analysis, the initial frequencies of oscillation of the two nuclei are chosen equal, $b = b_1 = b_2$, and $k_1 = k_2 = b$. The coupling gains, g_1 and g_2 in Fig. 1 are chosen to be equal and denoted as g in the following. Each node in the loop can be expressed, using phasor notation, with Z_1 the reference phasor, as

$$Z_1 = Y_m \tag{1}$$

$$Z_2 = D_1(Y_m) \cdot Y_m \tag{2}$$

$$Z_3 = D_1(Y_m) \cdot Y_m \cdot |G_1(j\omega)|\, e^{j\angle G_1(j\omega)} \tag{3}$$

$$Z_4 = Y_m e^{j\theta} \tag{4}$$

$$Z_5 = D_2(Y_m e^{j\theta}) \cdot Y_m e^{j\theta} \tag{5}$$

$$Z_6 = D_2(Y_m e^{j\theta}) \cdot Y_m e^{j\theta} \cdot |G_2(j\omega)|\, e^{j\angle G_2(j\omega)}. \tag{6}$$

From Fig. 1, with the coupling in the excitatory-inhibitory configuration as shown, it is clear that

$$Z_1 = Z_3 + gZ_6 \tag{7}$$

and

$$Z_4 = Z_6 - gZ_3. \tag{8}$$

Under the assumed conditions, the input signals at Z_1 and Z_4 are equal in amplitude and frequency, and $G_1(j\omega) = G_2(j\omega)$. The following equality, therefore, holds

$$D_1(Y_m) \cdot |G_1(j\omega)|\, e^{j\angle G_1(j\omega)} = D_2(Y_m e^{j\theta}) \cdot |G_2(j\omega)|\, e^{j\angle G_2(j\omega)}. \tag{9}$$

By letting M represent the complex number

$$M = D(Y_m)\, |G(j\omega)|\, e^{j\angle G(j\omega)}. \tag{10}$$

(7) reduces to

$$Y_m = MY_m + gMY_m e^{j\theta} \tag{11}$$

and (8) similarly can be expressed as

$$Y_m e^{j\theta} = MY_m e^{j\theta} - gMY_m. \tag{12}$$

Combining (11) and (12), and using Euler's formula yields

$$2g\cos\theta = 0 \tag{13}$$

giving

$$\theta = \pm\frac{\pi}{2}. \tag{14}$$

Substituting this value into either (11) or (12) results in

$$M = \frac{1}{\sqrt{1+g^2}} e^{j\arctan(\pm g)}. \tag{15}$$

Therefore, from (10) and (15)

$$\angle G(j\omega) = \arctan(\pm g). \tag{16}$$

From the definition of the second-order transfer function, shown in Fig. 1

$$\angle G(j\omega) = \frac{\pi}{2} - 2\arctan\left(\frac{\omega}{b}\right). \tag{17}$$

Rearranging gives

$$\omega = b\tan\left\{\frac{1}{2}\left[\frac{\pi}{2} - \arctan(\pm g)\right]\right\}. \tag{18}$$

Equation (18) thus defines the two new frequencies of oscillation that emerge as a function of the coupling gain g, and b, the original angular frequency of the oscillations, for the network topology shown in Fig. 1.

B. Fourth-Order Series Model (Reduced)

The fourth-order series model (reduced) comprises two reciprocally connected second-order nuclei, with transfer functions

$$G_r(s) = \frac{k}{(s+b)^2} \tag{19}$$

without the individual feedback connections included in the model described in Section II-A. The nuclei in this configuration are not capable of oscillating individually, but will begin to oscillate once the coupling gain between them reaches a critical value. High-frequency stimulation representative of DBS is also included. DBS is modeled here as a biphasic, rectangular waveform, with an amplitude of stimulation a and fractional pulse duration α, and is applied additively at the input to a nonlinear element, Fig. 2. This is analogous to adding the stimulation to the synaptic input of the neurons in the network, consistent with orthodromic driving of the neuron. As described in [40], the addition of this high-frequency stimulation to the system essentially counteracts the increase in the slope of the nonlinear element, and subsequent increased excitability, caused by a decrease in h_n, thereby suppressing the oscillatory activity induced. Experimental [48] and simulation [49] studies at the cellular level indicate that DBS does elicit its effect through antidromic and orthodromic activation of target neurons.

In order to analyze the fourth-order series model (reduced) shown in Fig. 2, the applied high-frequency stimulation, representative of DBS, is mathematically combined with the nonlinear element NL_1 resulting in an equivalent nonlinear element [50], [51]. As described in [40], describing function analysis techniques from [52] are applied to find a linear approximation of the gain of this equivalent nonlinear element, calculated as

$$D(Y_m) = \frac{4h_1}{\pi Y_m^2}\left(\sqrt{\frac{Y_m^2}{h_1^2}+1}-1\right) - \frac{8\alpha h_1}{\pi Y_m^2}\left(\sqrt{\frac{Y_m^2}{h_1^2}+1}-\frac{Y_m}{h_1}(f)\right) \quad (20)$$

where

$$f = \sqrt{\frac{\left(d^2+1-c^2\right)+\sqrt{\left(d^2+1-c^2\right)^2+4c^2d^2}}{2}} \quad (21)$$

and

$$c = \frac{a}{Y_m}\ ,\ d = \frac{h_1}{Y_m}.$$

The describing function of the original nonlinearity, NL_2, is denoted D_o, with D_e the notation assigned to the describing function of the equivalent nonlinearity, $NL_1 + DBS$. The amplitude of the oscillations is described at each given point in the loop in terms of the describing function as follows:

$$X_1 = D_o(Y_m)\cdot Y_m \quad (22)$$

$$X_2 = D_o(Y_m)\cdot Y_m \cdot |G_r(jb)| \quad (23)$$

$$X_3 = D_o(Y_m)\cdot Y_m \cdot |G_r(jb)| \cdot D_e(D_o(Y_m)\cdot Y_m \cdot |G_r(jb)|) \quad (24)$$

$$X_4 = D_o(Y_m)\cdot Y_m \cdot |G_r(jb)| \cdot D_e(D_o(Y_m)\cdot Y_m \cdot |G_r(jb)|)\cdot |G_r(jb)|\,. \quad (25)$$

From Fig. 2, it is clear that in (25) $X_4 = Y_m$, and so

$$D_o(Y_m)\cdot D_e(D_o(Y_m)\cdot Y_m \cdot |G_r(jb)|) = \frac{1}{|G_r(jb)|\,|G_r(jb)|}. \quad (26)$$

Allowing both transfer functions to be equal, as given in (19), and evaluating at angular frequency b yields

$$|G_r(jb)| = \frac{k}{2b^2}. \quad (27)$$

Combining this with (26) gives

$$\frac{1}{|G_r(jb)|\,|G_r(jb)|} = \frac{4b^4}{k^2} \quad (28)$$

which sets the critical value of the composition of describing functions to that for which oscillations will occur in the fourth-order series model (reduced). Letting $k = b^2$ in (28) results in a threshold value, to ascertain whether oscillatory activity is present in the system, equal to 4. For oscillations to occur in the system, the phase condition must also be satisfied; that is, the phase difference around the feedback loop must sum to zero. Each transfer function contributes a phase difference of $-\frac{\pi}{2}$, and when combined with the negative feedback in the model yields a total phase difference of zero.

In order to examine the effects of changing the parameters and the stimulation applied to the model on the amplitude of the oscillations, the intersection point between the describing function and the threshold for generation of oscillations is calculated for a range of parameter values. First, the amplitude of oscillations, denoted Y_m, is calculated as a function of h_1, the parameter modeling the effect of dopamine on the system. Stimulation is then applied to the system and the effect of varying a, the amplitude of applied stimulation, α, the fractional pulse duration of the applied stimulation and the frequency of the stimulation on the oscillations in the system for a fixed value of h_1 is examined.

C. Clinical Data

To verify the behavior of the model in comparison to the physiological system, the model parameters of the fourth-order series model (reduced) were optimized to fit clinical LFP data recorded postoperatively. The data were recorded at the Department of Clinical Neurology, University of Oxford, and at the University College of London, from four patients with Parkinson's disease who had undergone bilateral implantation of DBS electrodes into the STN. All patients gave their informed consent to take part in the study, which was approved by the local ethics committees of the University of Oxford or University College of London. The permanent quadripolar macroelectrode implanted was model 3387 (Medtronic Neurologic Division, Minneapolis, MN, USA). Bipolar LFPs were captured using a single channel, isolated, high-gain (100 dB) amplifier with a pass band of 4–40 Hz from contact pairs 0–2 or 1–3 (contact 0 being the most caudal and contact 3 the most rostral contact) and recorded onto a PC via a 1401 data acquisition system (Cambridge Electronic Design Ltd., Cambridge, U.K.). Data were recorded with a sampling frequency of 2.2 kHz, except in one patient where a sampling rate of 200 Hz was used. Recordings were obtained after overnight withdrawal from patients' usual antiparkinsonian medication while the patients sat comfortably in a chair. Patients were stimulated monopolarly at either contact 1 (if the LFP was captured from contacts 0–2) or contact 2 (if the LFP was captured from contacts 1–3). Stimulation and recording contact pairs were determined according to which bipolar LFP contacts exhibited highest beta power. To determine this, two short recordings of 100 s were made in the absence of stimulation from contact pairs 0–2 and 1–3. Power spectral density was calculated offline using Spike2 (Cambridge Electronic Design Ltd., Cambridge, U.K.). Based on this assessment, for each patient the LFPs were recorded as the stimulation amplitude, delivered via the external stimulator (Medtronic Neurologic Division, Minneapolis, MN, USA), was varied while the stimulation frequency and pulse duration were kept fixed, at 130 Hz and either 60 or 90 μs, respectively.

The raw data were imported from Spike2 (Cambridge Electronic Design Ltd., Cambridge, U.K.) and processed using custom developed software (MATLAB 7.12, The MathWorks Inc., Natick, MA, USA, 2011). Each dataset was filtered using a tenth-order Butterworth filter with cutoff frequencies $13 < f < 35$ Hz in order to examine the data in the beta frequency range. To calculate the amplitude of the oscillations for each stimulation setting, the root mean square (RMS) value of 5 s epochs, with an 80% overlap, were calculated. In each case, the epochs were chosen to begin 10 s after the adjustment to the stimulation took place. The amplitude of the beta-band oscillations in the LFP data for each stimulation setting was calculated as the average of the 5 s RMS values, converted to

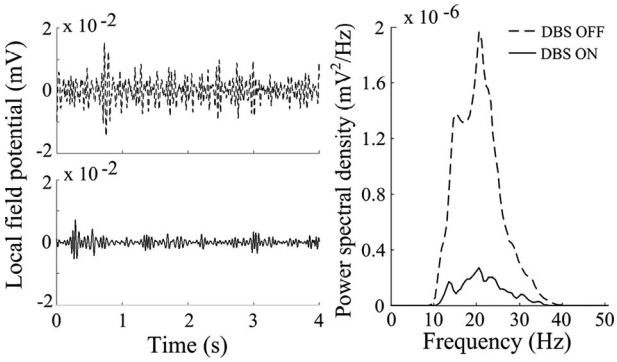

Fig. 3. Sample of LFP data recorded via implanted macroelectrodes from the STN of a patient with Parkinson's disease shown before stimulation was applied and during 130-Hz stimulation at 1.5 V with a pulse duration of 60 μs. The power spectrum shown, estimated using Welch's method, is based on the entire LFP recording for the given stimulation settings.

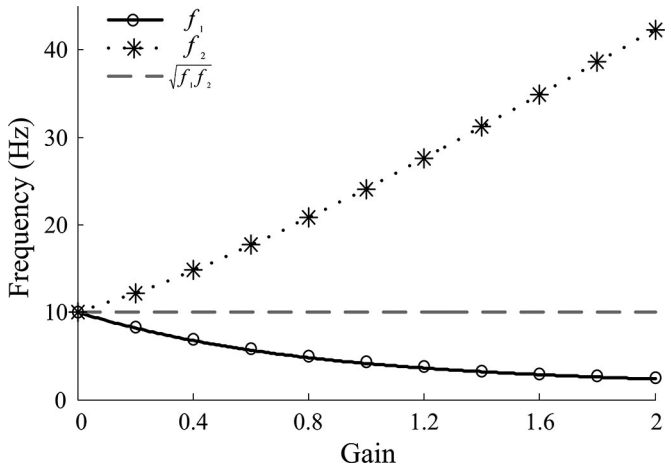

Fig. 4. Diverging frequencies (f_1 and f_2) of the fourth-order series model (with feedback) as a function of coupling gain. f_1 and f_2 denote a frequency component of the oscillatory activity. Both ensembles are initialized to oscillate at 10 Hz, with the model in the excitatory-inhibitory configuration. The theoretically predicted frequencies based on (18) are shown, as well as the frequency of the output from simulations of the system for discrete values of coupling gain. The geometric mean of the two frequencies, $\sqrt{f_1 f_2}$, remains approximately constant and is also illustrated. Note that a single frequency can give rise to any value.

beta-band power, and was normalized with respect to the DBS-off data recorded during that trial. Two samples of the filtered LFP data are shown in Fig. 3—both before stimulation and during 130 Hz stimulation applied at an amplitude of 1.5 V and a pulse duration of 60 μs.

D. Model Analysis

In addition to the theoretical analysis, both of the fourth-order series models were implemented and simulated using a commercial software package (Simulink, MATLAB 7.12, The MathWorks Inc., Natick, MA, USA, 2011).

In order to fit the theoretical output of the fourth-order series model (reduced) to the clinical data, the model parameters were optimized to fit each individual dataset using the Levenberg–Marquardt algorithm to minimize the difference between the power of the clinically recorded LFP data and the model estimates of the oscillation power. The R^2 values, indicating the agreement between the model predictions and the clinical data, were calculated for each fitted dataset. This procedure was repeated with the previously presented second-order model [40] and the same sets of clinical data to enable a comparison to be drawn between the two models.

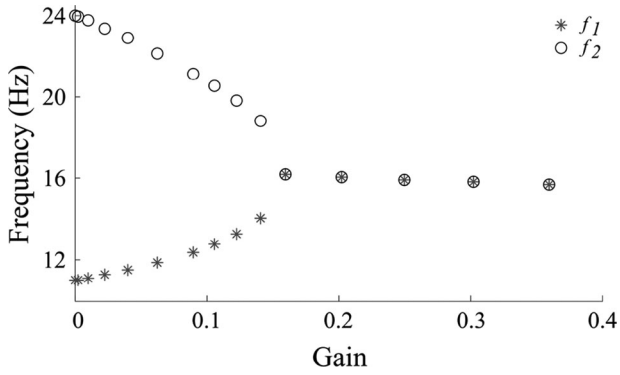

Fig. 5. Converging frequencies (f_1 and f_2) of the coupled fourth-order series model (with feedback) as a function of coupling gain. f_1 and f_2 denote a frequency component of the oscillatory activity. The frequencies converge to their geometric mean, and then decrease with increasing gain. The points illustrated were obtained through simulation of the system shown in Fig. 1, with the networks set to initially oscillate at two different frequencies (11 and 24 Hz), with the coupling between the networks in the excitatory-excitatory configuration.

III. Results

A. Fourth-Order Series Model (With Feedback)

The effect of increasing the amplitude of the coupling gain in the fourth-order series model (with feedback), Fig. 1, is illustrated in Figs. 4 and 5. Fig. 4 shows the frequencies present as a function of coupling gain when both ensembles are initialized to oscillate at the same frequency (10 Hz), with excitatory-inhibitory coupling of the model. This is achieved by taking $h_1 = 0.3$ and $b = 5\pi$. Both the theoretically predicted frequencies based on (18), and frequencies measured from the output of the simulated system for discrete values of gain are presented. As the coupling gain in the network is increased, the frequencies diverge, with this behavior also observed in the model simulations. The geometric mean of the frequencies, which is illustrated in Fig. 4, remains approximately constant.

Fig. 5 illustrates the frequencies of the simulated model output obtained when the individual networks shown in Fig. 1 are initialized to oscillate at different frequencies (11 and 24 Hz), again as the amplitude of the coupling gain is increased. This is achieved by setting $b_1 = 5.5\pi$ and $b_2 = 12\pi$. The two frequencies are observed to converge towards an intermediate frequency with increasing gain. When the frequencies converge, the single resultant frequency decreases gradually as the gain is increased further. These results are based on simulations of the system shown in Fig. 1 with the excitatory-excitatory system configuration used, $g_1 = -g_2$.

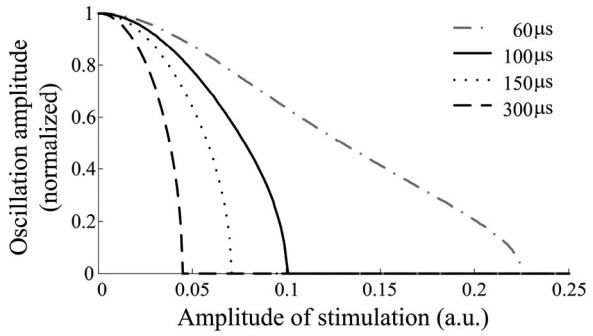

Fig. 6. Amplitude of oscillations (normalized values) in the fourth-order series model (reduced) of neural synchrony as a function of the amplitude of applied stimulation, given in arbitrary units (a.u.). Four different pulse durations of stimulation are presented. h_1 is chosen to be 0.1 in each.

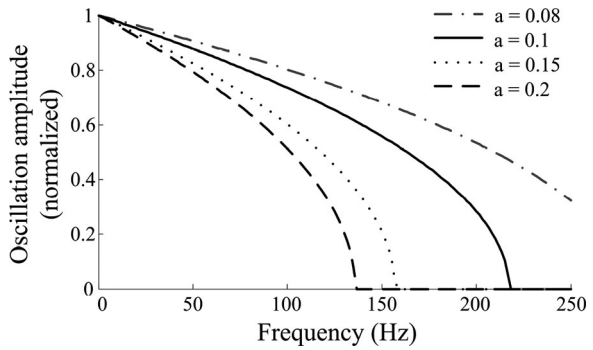

Fig. 7. Amplitude of oscillations (normalized values) in the fourth-order series model (reduced) of neural synchrony as a function of the frequency of applied stimulation. Four different amplitudes of stimulation are presented. h_1 is chosen to be 0.1 in each.

B. Fourth-Order Series Model (Reduced)

The describing function analysis developed here enables the amplitude of the oscillations present in the system to be calculated as a function of the parameter h_1, representing the dopamine level in the system. The oscillations increased in amplitude as the parameter h_1 was decreased. The amplitude of oscillations in the model for any particular fixed value of h_1 can be evaluated analytically for a range of applied stimulation parameters, as shown in Figs. 6 and 7. In each case, the amplitude of oscillations present in the system is shown normalized with respect to the amplitude without stimulation applied. In Fig. 6, the amplitude of oscillations are plotted as a function of the amplitude of the applied stimulation, a, for four separate pulse durations. The amplitude of the oscillations is decreased as the amplitude of the stimulation is increased, with the oscillations suppressed more readily as the pulse duration is increased. Fig. 7 shows the amplitude of oscillations within the series network plotted as a function of frequency for four different amplitudes of stimulation. The amplitude of the oscillations is decreased as the frequency of the applied stimulation is increased. The suppression achieved is increased as the amplitude of the applied stimulation is increased. In each case, $h_1 = 0.1$.

TABLE I
OPTIMAL PARAMETERS OF THEORETICAL SECOND-ORDER MODEL IDENTIFIED TO FIT PREDICTIONS TO LFP DATA FROM FOUR PATIENTS SHOWN IN FIG. 8(A)

Patient	#1	#2	#3	#4
h	0.3167	0.3170	0.3177	0.3180
Scaling on x-axis	7.42	53.28	37.36	65.97
Scaling on y-axis	0.0022	0.0016	0.0008	0.0004
Pulse duration of stim. (μs)	60	90	60	60
Frequency of stim. (Hz)	130	130	130	130

The pulse duration and frequency of the stimulation applied in each case is also included.

TABLE II
OPTIMAL PARAMETERS OF THEORETICAL FOURTH-ORDER SERIES MODEL (REDUCED) IDENTIFIED TO FIT LFP DATA FROM FOUR PATIENTS SHOWN IN FIG. 8(B)

Patient	#1	#2	#3	#4
h_1	0.1011	0.0999	0.1008	0.1011
Scaling on x-axis	44.66	91.25	71.25	151.74
Scaling on y-axis	0.0001	0.0005	0.0002	0.0001
Pulse duration of stim. (μs)	60	90	60	60
Frequency of stim. (Hz)	130	130	130	130

The pulse duration and frequency of the stimulation applied in each case is also included.

C. Comparison of Models with Experimental Data

The parameters of the original second-order model and the fourth-order series model (reduced) were optimized for each patient independently. The model parameters and stimulation settings identified for each dataset are given in Table I and Table II, and the experimental and theoretically predicted data are compared in Fig. 8. The amplitude of oscillations in the experimental dataset are normalized with respect to the off-DBS recording for that patient. In each case, the pulse duration was fixed at either 60 or 90 μs as the amplitude of the stimulation was varied.

IV. DISCUSSION

It is hypothesized that the healthy basal ganglia consists of functionally distinct networks that lose their segregation under conditions of dopamine depletion, leading to pathological oscillatory activity [7], [8]. Amassed evidence from the literature supports the proposal that the pathological oscillations observed in Parkinson's disease arise as a result of the interaction of two or more populations of synchronized neurons. In this study, control theory has been used in order to gain insight into the generation and interaction of oscillatory activity in two simplified network models each representing two interacting populations of neurons.

Specifically, describing function analysis provides a method of exploring and understanding the oscillatory activity in both of the fourth-order series models of neural synchrony presented in this study, including the effect of applying high-frequency stimulation to the oscillations produced. The method of combining two describing functions is a novel approach, which allows the application of the well-established engineering tool

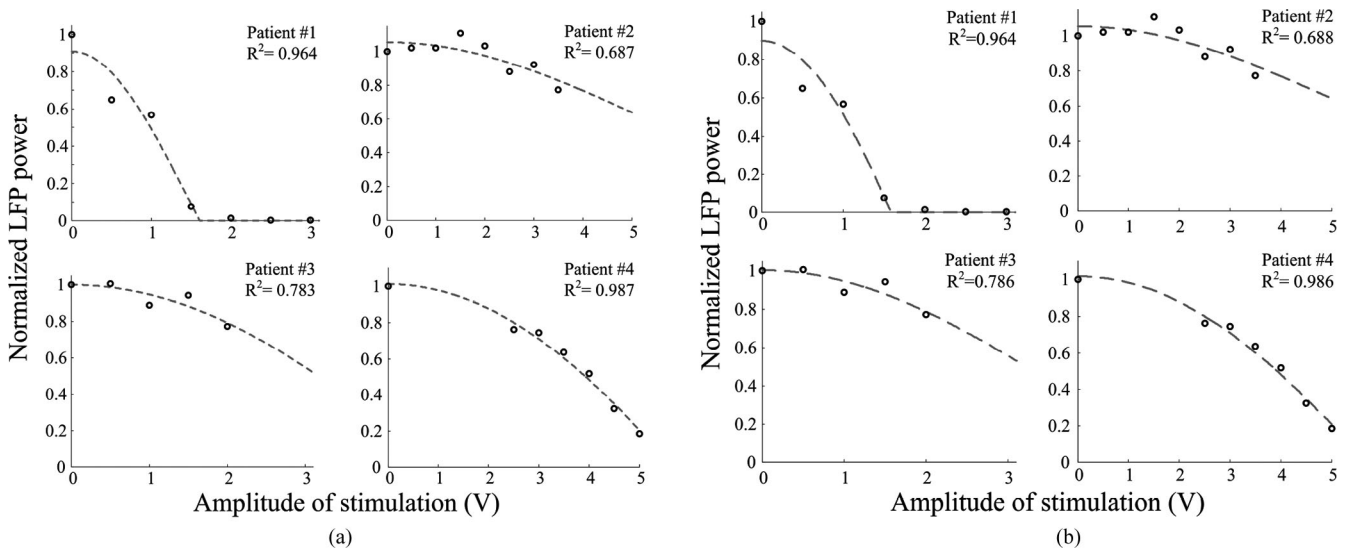

Fig. 8. Normalized LFP beta-band power as a function of the amplitude of applied stimulation for the theoretical models of synchronous neural activity, optimized to fit four experimental patient datasets. The patient data are shown (○) along with the theoretical fit to the model optimized for that individual patient as the DBS amplitude is increased. The stimulation frequency was fixed at 130 Hz, and the pulse duration at 60 μs, except for Patient #2, where a pulse duration of 90 μs was used. The R^2 value calculated for each fit is also included. (a) Second-order model of synchronous neural activity. (b) Fourth-order series model (reduced) of synchronous neural activity.

to the fourth-order series models presented. This method can also be extended to the analysis of higher order models with a greater number of interacting nuclei, which may provide a more accurate representation of the physiological system in question, while still remaining analytically tractable. Although the method of describing function analysis was the one chosen and applied here, other techniques such as bifurcation analysis could equally be utilized in order to characterize the oscillatory activity of the models presented here.

The analysis of the fourth-order series model (with feedback) explores how the output frequency or frequencies of the produced oscillatory activity depend on the coupling gain of the model. For reciprocally connected loops of two oscillating interconnected networks, with excitatory-inhibitory interconnections, initialized to oscillate at the same frequency, two divergent frequencies emerge as the coupling gain between the nuclei is increased. The geometric mean of these two frequencies remains approximately constant; see Fig. 4. When the coupled loops are set to oscillate at different initial frequencies, with excitatory-excitatory interconnections, the frequencies converge as the coupling gain is increased. As the gain is increased above that at which the frequencies converge, this resultant frequency decreases slightly from that of the initial convergence point; see Fig. 5. Similar results were demonstrated with a more physiologically detailed study of the cortico-basal ganglia-thalamocortical network [31], where the interaction of oscillations at different frequencies in the cortex and STN were examined and found to result in a new, intermediate frequency of synchronized oscillations under dopamine depleted conditions (increased coupling gain). The geometric mean of the converging frequencies was also observed to remain approximately constant [31].

Oscillatory activity recorded from the cortico-basal ganglia-thalamocortical network has been shown to occur at a range of frequencies. Given the increased functional connectivity between these loops that occurs in Parkinson's disease [9], it is likely that interaction between loops of different frequencies does occur. The measured LFP likely reflects activity generated by synchronous synaptic inputs to the STN, including afferent inputs from the cortex through the hyperdirect pathway, along with inputs from the GPe and other interconnecting nuclei. In [53], bispectral analysis of LFP data recorded from the STN of Parkinsonian patients revealed a nonlinear correlative relationship between LFP rhythms of different frequencies, which was decreased after dopaminergic medication. Marceglia *et al.* suggested that the loss of dopamine in Parkinson's disease causes a loss of segregation between different LFP rhythms [53], and that the nonlinear interactions observed could arise as a result of the synchronization between two or more populations of neurons [54]. In particular, overactivity in the hyperdirect pathway has been postulated as playing a critical part in the generation of the pathological oscillations associated with Parkinson's disease [13], [14], [55]. The theoretical and simulated results presented here suggest some possible mechanisms by which the pathological oscillatory activity observed in Parkinson's disease may occur via a similar loss of segregation or increased coupling gain between the individual nuclei. The results in Fig. 5 show how frequencies in the low beta range (16 Hz) can be produced by combining 11 and 24 Hz oscillations in two separate networks and increasing the coupling gain. Similarly, two diverging frequencies of oscillation are shown to emerge from the series with feedback network arrangement of two nuclei with initially equal frequencies of oscillation, illustrated for 10 Hz; see Fig. 4.

The fourth-order series model (reduced), representative of two synchronous nuclei, predicts oscillatory activity that grows in amplitude as the parameter h_1 is decreased causing an increase in the excitability of the loop. For any chosen frequency

and initial amplitude of oscillations, the theoretical analysis predicts that the oscillatory activity decreases in amplitude as either the frequency, pulse duration, or amplitude of the applied stimulation, representing DBS, is increased; see Figs. 6 and 7. The suppression of oscillations in this way can also be described as a supercritical Hopf bifurcation. As the amplitude of applied stimulation is increased the stable oscillations in the system disappear. This description of the changes in dynamics induced in an oscillatory network by the application of high-frequency stimulation as a Hopf bifurcation was first observed by Titcombe *et al.* [34].

The theoretical results of varying amplitude of stimulation for fixed frequency and pulse duration were fitted to clinically recorded LFP data from four individual Parkinsonian patients using optimization, with the R^2 values calculated as 0.96, 0.69, 0.79, and 0.99, respectively, indicating a good agreement between the model and the clinical values. The output of the original second-order model explored in [40] was fitted to the same clinically recorded LFP datasets. The R^2 values of this fit were calculated as 0.96, 0.69, 0.78, and 0.99. The similarity between the fits obtained to the clinical data for both the second- and fourth-order models indicate that the addition of a second nucleus to the network does not improve the accuracy of the model in representing the dynamics of the Parkinsonian LFP in the datasets examined. Indeed, the second-order model examined in our earlier study [40], and a third-order model described in a study by Titcombe *et al.* [34], have been shown to accurately capture the dynamics of a clinical data set obtained from the literature [41].

A decrease in h_1 in the model is analogous to the depletion of dopamine in Parkinson's disease, with the resulting increased amplitude of the oscillatory activity mimicking that observed in LFP data recorded from the pathological basal ganglia. An improvement in motor symptoms in patients is seen to occur in parallel with either a drug, or DBS-induced, suppression of this oscillatory activity [15], [18], [19], [21]. Furthermore, clinical studies report a progressive improvement in the motor symptoms of the disease as the amplitude, and to a lesser extent, the frequency and pulse duration, of the applied DBS is increased [56]–[58]. As a causal relationship between a decrease in beta-band oscillations and motor symptom reduction has not yet been proven, the suppression of the oscillatory activity in the model with high-frequency stimulation cannot be taken as translating directly into a clinical improvement in the motor symptoms. However, evidence from recent studies lends weight to the use of the beta-band oscillatory activity as a biomarker of the disease, which supports this representation.

Mathematical models of the cortico-basal ganglia-thalamocortical region provide a pathway to further understanding of the underlying pathological oscillatory activity of Parkinson's disease. Using models, hypotheses can be easily tested, developed and refined. Comparisons can be made between models of differing levels of complexity in addition to direct comparisons with clinical data, where model complexity allows. The models presented in this study have the advantage of being easily manipulated and analytically tractable. This may facilitate their translation to a clinical environment where they could be used as a tool to aid in the choice of stimulation parameters. They can be tuned to match individual patient disease characteristics—the model parameters b, k, and h_1 can be chosen to tune the output to whatever the dominant frequency and amplitude of oscillation recorded from the patient is. The stimulation parameters can then be chosen based on the level of suppression required, although it is likely, due to the interpatient variability observed in LFP data [8], that the suppression required may be patient specific. Translation of the model to a clinical environment would involve restricting the optimization of the model parameters to a certain area of the parameter space in order to comply with clinically safe levels of stimulation, and to minimize side effects. This method could also be extended to include tuning of the model using alternative, more readily recordable potential biomarkers of Parkinson's disease, for example, electromyography or limb tremor. Although the focus in this study is on beta-band oscillations in two interacting nuclei, the models presented can also be extended to include a number of nuclei oscillating at a range of different frequencies based on physiological recordings, and used to study the interaction of these as the gain of the system is increased, mimicking the increased functional connectivity that occurs with the depletion of dopamine. The theoretical analyses outlined can be extended to higher order models based on combinations of the two basic network architectures presented in this study.

The models presented here represent two interacting nuclei displaying synchronous oscillatory dynamics. This is based on the hypothesis that the pathological oscillatory activity observed in Parkinson's disease arises as a result of the loss of functional segregation in the basal ganglia-thalamocortical system. However, the reduction of the system to include just two subnetworks may well be an oversimplification. In addition, although the models presented in this study provide good agreement with the clinically recorded LFP data, it is important to note that, as mean-field type models, much physiological accuracy and detail is neglected, and therefore, some of the effect of the subtle relationships and interactions between neurons are lost. Similarly, the stimulation representing DBS is applied additively at the input to one nuclei, with no consideration given to the interaction of the stimulation pulse with the tissue surrounding the electrode. Finally, the use of the describing function analysis is an approximation method, however, its application to models presented here is justified by ensuring the appropriate specifications are met in the model, and by confirming the theoretical results achieved through simulation of the model.

V. Conclusion

Mathematical models of the cortico-basal ganglia-thalamocortical network that capture the key features of the physiological system in order to produce a faithful representation of the dynamics, while remaining analytically tractable, are particularly valuable. The results presented in this study demonstrate that both the second-order and fourth-order series (reduced) models provide close agreement between the model output and clinical data. Therefore the second-order model is sufficient to represent the system, with the added complexity of

the fourth-order model, in this case, unnecessary. The agreement observed offers the possibility that the model could be translated to a clinical tool to aid in DBS parameter selection. The model could conceivably be tuned to represent an individual patients pathological state using a biomarker of Parkinson's disease. The analytically tractable theoretical analysis established here can readily be extended to higher order models also, thus providing a valuable framework with which to examine and test new models of this type.

REFERENCES

[1] J.-S. Brittain and P. Brown, "Oscillations and the basal ganglia: Motor control and beyond," *Neuroimage*, vol. 85, pp. 637–647, 2014.

[2] A. K. Engel and P. Fries, "Beta-band oscillations—Signalling the status quo?" *Current Opinion Neurobiol,*, vol. 20, no. 2, pp. 156–165, 2010.

[3] R. Joundi, N. Jenkinson, J.-S. Brittain, T. Aziz, and P. Brown, "Driving oscillatory activity in the human cortex enhances motor performance," *Current Biol.*, vol. 22, no. 5, pp. 403–407, 2012.

[4] T. Koelewijn, H. T. van Schie, H. Bekkering, R. Oostenveld, and O. Jensen, "Motor-cortical beta oscillations are modulated by correctness of observed action," *NeuroImage*, vol. 40, no. 2, pp. 767–775, 2008.

[5] C. Hammond, H. Bergman, and P. Brown, "Pathological synchronization in Parkinson's disease: Networks, models and treatments," *Trends Neurosci.*, vol. 30, no. 7, pp. 357–364, 2007.

[6] H. Bergman, A. Feingold, A. Nini, A. Raz, H. Slovin, M. Abeles, and E. Vaadia, "Physiological aspects of information processing in the basal ganglia of normal and Parkinsonian primates," *Trends Neurosci.*, vol. 21, no. 1, pp. 32–38, 1998.

[7] J. Dostrovsky and H. Bergman, "Oscillatory activity in the basal ganglia—Relationship to normal physiology and pathophysiology," *Brain*, vol. 127, no. 4, pp. 721–722, 2004.

[8] H. Bronte-Stewart, C. Barberini, M. M. Koop, B. C. Hill, J. M. Henderson, and B. Wingeier, "The STN beta-band profile in Parkinson's disease is stationary and shows prolonged attenuation after deep brain stimulation," *Exp. Neurol.*, vol. 215, no. 1, pp. 20–28, 2009.

[9] S. Baudrexel, T. Witte, C. Seifried, F. von Wegner, F. Beissner, J. C. Klein, H. Steinmetz, R. Deichmann, J. Roeper, and R. Hilker, "Resting state fMRI reveals increased subthalamic nucleus motor cortex connectivity in Parkinson's disease," *NeuroImage*, vol. 55, no. 4, pp. 1728–1738, 2011.

[10] A. Kumar, S. Cardanobile, S. Rotter, and A. Aertsen, "The role of inhibition in generating and controlling Parkinson's disease oscillations in the basal ganglia," *Front. Syst. Neurosci.*, vol. 5, art. 86, pp. 1–14, 2011.

[11] A. C. Marreiros, H. Cagnan, R. J. Moran, K. J. Friston, and P. Brown, "Basal ganglia-cortical interactions in Parkinsonian patients," *NeuroImage*, vol. 66, pp. 301–310, 2012.

[12] J. Hirschmann, T. Ozkurt, M. Butz, M. Homburger, S. Elben, C. Hartmann, J. Vesper, L. Wojtecki, and A. Schnitzler, "Distinct oscillatory STN-cortical loops revealed by simultaneous MEG and local field potential recordings in patients with Parkinson's disease," *NeuroImage*, vol. 55, no. 3, pp. 1159–1168, 2011.

[13] R. J. Moran, N. Mallet, V. Litvak, R. J. Dolan, P. J. Magill, K. J. Friston, and P. Brown, "Alterations in brain connectivity underlying beta oscillations in Parkinsonism," *PLoS Comput. Biol.*, vol. 7, no. 8, pp. e1002124-1–e1002124-15, 2011.

[14] V. Gradinaru, M. Mogri, K. R. Thompson, J. M. Henderson, and K. Deisseroth, "Optical deconstruction of Parkinsonian neural circuitry," *Science*, vol. 324, no. 5925, pp. 354–359, 2009.

[15] A. A. Kuhn, F. Kempf, C. Brucke, L. Gaynor Doyle, I. Martinez-Torres, A. Pogosyan, T. Trottenberg, A. Kupsch, G.-H. Schneider, M. I. Hariz, W. Vandenberghe, B. Nuttin, and P. Brown, "High-frequency stimulation of the subthalamic nucleus suppresses oscillatory beta activity in patients with Parkinson's disease in parallel with improvement in motor performance," *J. Neurosci.*, vol. 28, no. 24, pp. 6165–6173, 2008.

[16] N. Ray, N. Jenkinson, S. Wang, P. Holland, J. Brittain, C. Joint, J. Stein, and T. Aziz, "Local field potential beta activity in the subthalamic nucleus of patients with Parkinson's disease is associated with improvements in bradykinesia after dopamine and deep brain stimulation," *Exp. Neurol.*, vol. 213, no. 1, pp. 108–113, 2008.

[17] P. Tass, D. Smirnov, A. Karavaev, U. Barnikol, T. Barnikol, I. Adamchic, C. Hauptmann, N. Pawelcyzk, M. Maarouf, V. Sturm, H.-J. Freund, and B. Bezruchko, "The causal relationship between subcortical local field potential oscillations and Parkinsonian resting tremor," *J. Neural Eng.*, vol. 7, no. 1, pp. 016009-1–016009-16, 2010.

[18] P. Brown, A. Oliviero, P. Mazzone, A. Insola, P. Tonali, and V. Di Lazzaro, "Dopamine dependency of oscillations between subthalamic nucleus and pallidum in Parkinson's disease," *J. Neurosci.*, vol. 21, no. 3, pp. 1033–1038, 2001.

[19] A. Priori, G. Foffani, A. Pesenti, F. Tamma, A. Bianchi, M. Pellegrini, M. Locatelli, K. Moxon, and R. Villani, "Rhythm-specific pharmacological modulation of subthalamic activity in Parkinson's disease," *Exp. Neurol.*, vol. 189, no. 2, pp. 369–379, 2004.

[20] M. Beudel, S. Little, A. Pogosyan, K. Ashkan, T. Foltynie, P. Limousin, L. Zrinzo, M. Hariz, M. Bogdanovic, B. Cheeran, A. L. Green, T. Aziz, W. Thevathasan, and P. Brown, "Tremor reduction by deep brain stimulation is associated with gamma power suppression in Parkinson's disease," *Neuromodulation: Technol. Neural Interface*, vol. 18, pp. 394–354, 2015.

[21] P. Silberstein, A. Pogosyan, A. A. Khn, G. Hotton, S. Tisch, A. Kupsch, P. Dowsey-Limousin, M. I. Hariz, and P. Brown, "Cortico-cortical coupling in Parkinson's disease and its modulation by therapy," *Brain*, vol. 128, no. 6, pp. 1277–1291, 2005.

[22] M. Alegre and M. Valencia, "Oscillatory activity in the human basal ganglia: More than just beta, more than just Parkinson's disease," *Exp. Neurol.*, vol. 248, pp. 183–186, 2013.

[23] S. Little, A. Pogosyan, A. Kuhn, and P. Brown, "Beta band stability over time correlates with Parkinsonian rigidity and bradykinesia," *Exp. Neurol.*, vol. 236, no. 2, pp. 383–388, 2012.

[24] J. E. Rubin and D. Terman, "High frequency stimulation of the subthalamic nucleus eliminates pathological thalamic rhythmicity in a computational model," *J. Comput. Neurosci.*, vol. 16, pp. 211–235, 2004.

[25] M. Pirini, L. Rocchi, M. Sensi, and L. Chiari, "A computational modelling approach to investigate different targets in deep brain stimulation for Parkinson's disease," *J. Comput. Neurosci.*, vol. 26, pp. 91–107, 2009.

[26] X.-J. Feng, E. Shea-Brown, B. Greenwald, R. Kosut, and H. Rabitz, "Optimal deep brain stimulation of the subthalamic nucleus: A computational study," *J. Comput. Neurosci.*, vol. 23, pp. 265–282, 2007.

[27] A. D. Dorval, A. M. Kuncel, M. J. Birdno, D. A. Turner, and W. M. Grill, "Deep brain stimulation alleviates Parkinsonian bradykinesia by regularizing pallidal activity," *J. Neurophysiol.*, vol. 104, no. 2, pp. 911–921, 2010.

[28] M. D. Humphries, R. D. Stewart, and K. N. Gurney, "A physiologically plausible model of action selection and oscillatory activity in the basal ganglia," *J. Neurosci.*, vol. 26, no. 50, pp. 12 921–12 942, 2006.

[29] T. Otsuka, T. Abe, T. Tsukagawa, and W.-J. Song, "Conductance-based model of the voltage-dependent generation of a plateau potential in subthalamic neurons," *J. Neurophysiol.*, vol. 92, no. 1, pp. 255–264, 2004.

[30] P. J. Hahn and C. C. McIntyre, "Modeling shifts in the rate and pattern of subthalamopallidal network activity during deep brain stimulation," *J. Comput. Neurosci.*, vol. 28, no. 3, pp. 425–441, 2010.

[31] G. Kang and M. Lowery, "Interaction of oscillations, and their suppression via deep brain stimulation, in a model of the cortico-basal ganglia network," *IEEE Trans. Neural Syst. Rehabilitation Eng.*, vol. 21, no. 2, pp. 244–253, Mar. 2013.

[32] A. B. Holt and T. I. Netoff, "Origins and suppression of oscillations in a computational model of Parkinson's disease," *J. Comput. Neurosci.*, vol. 37, pp. 1–17, 2014.

[33] H. R. Wilson and J. D. Cowan, "Excitatory and inhibitory interactions in localized populations of model neurons," *Biophys. J.*, vol. 12, no. 1, pp. 1–24, 1972.

[34] M. S. Titcombe, L. Glass, D. Guehl, and A. Beuter, "Dynamics of Parkinsonian tremor during deep brain stimulation," *Chaos: Interdisciplinary J. Nonlinear Sci.*, vol. 11, no. 4, pp. 766–773, 2001.

[35] A. J. N. Holgado, J. R. Terry, and R. Bogacz, "Conditions for the generation of beta oscillations in the subthalamic nucleus–Globus pallidus network," *J. Neurosci.*, vol. 30, no. 37, pp. 12 340–12 352, 2010.

[36] P. A. Tass and M. Majtanik, "Long-term anti-kindling effects of desynchronizing brain stimulation: A theoretical study," *Biol. Cybern.*, vol. 94, no. 1, pp. 58–66, 2006.

[37] C. Hauptmann and P. A. Tass, "Therapeutic rewiring by means of desynchronizing brain stimulation," *Biosystems*, vol. 89, no. 1–3, pp. 173–181, 2007.

[38] J.-P. Pfister and P. A. Tass, "STDP in oscillatory recurrent networks: Theoretical conditions for desynchronization and applications to deep brain stimulation," *Front. Comput. Neurosci.*, vol. 4, art. 22, pp. 1–10, 2010.

[39] S. J. Schiff, "Towards model-based control of Parkinson's disease," *Philos. Trans. Roy. Soc. London A, Math. Phys. Sci..*, vol. 368, no. 1918, pp. 2269–2308, 2010.

[40] C. Davidson, A. de Paor, and M. Lowery, "Application of describing function analysis to a model of deep brain stimulation," *IEEE Trans. Biomed. Eng.*, vol. 61, no. 3, pp. 957–965, Mar. 2014.
[41] A. Benabid, P. Pollak, D. Hoffmann, C. Gervason, M. Hommel, J. Perret, J. de Rougemont, and D. Gao, "Long-term suppression of tremor by chronic stimulation of the ventral intermediate thalamic nucleus," *Lancet*, vol. 337, no. 8738, pp. 403–406, 1991.
[42] D. Plenz and S. T. Kital, "A basal ganglia pacemaker formed by the subthalamic nucleus and external globus pallidus," *Nature*, vol. 400, pp. 677–682, 1999.
[43] G. Tsirogiannis, G. Tagaris, D. Sakas, and K. Nikita, "A population level computational model of the basal ganglia that generates Parkinsonian local field potential activity," *Biol. Cybern.*, vol. 102, no. 2, pp. 155–176, 2010.
[44] G. Buzsaki, C. A. Anastassiou, and C. Koch, "The origin of extracellular fields and currents—EEG, ECoG, LFP and spikes," *Nature Rev. Neurosci.*, vol. 13, no. 6, pp. 407–420, 2012.
[45] G. Deco, V. K. Jirsa, P. A. Robinson, M. Breakspear, and K. Friston, "The dynamic brain: From spiking neurons to neural masses and cortical fields," *PLoS Comput. Biol.*, vol. 4, no. 8, pp. 1–35, 2008.
[46] M. DeLong and T. Wichmann, "Circuits and circuit disorders of the basal ganglia," *Archives Neurol.*, vol. 64, no. 1, pp. 20–24, 2007.
[47] C. Dejean, C. E. Gross, B. Bioulac, and T. Boraud, "Dynamic changes in the cortex-basal ganglia network after dopamine depletion in the rat," *J. Neurophysiol.*, vol. 100, no. 1, pp. 385–396, 2008.
[48] R. Carron, A. Chaillet, A. Filipchuk, W. Pasillas-Lepine, and C. Hammond, "Closing the loop of deep brain stimulation," *Front. Syst. Neurosci.*, vol. 7, art. 112, pp. 1–18, 2013.
[49] G. Kang and M. M. Lowery, "Effects of antidromic and orthodromic activation of STN afferent axons during DBS in Parkinson's disease: a simulation study," *Front. Comput. Neurosci.*, vol. 8, art. 32, pp. 1–12, 2014.
[50] O. I. Elgerd, *Control Systems Theory*. New York, NY, USA: McGraw-Hill, 1967.
[51] C. Davidson, M. Lowery, and A. de Paor, "Application of non-linear control theory to a model of deep brain stimulation," in *Proc. IEEE Annu. Int. Conf. Eng. Med. Biol. Soc.*, Aug. 30–Sep. 3 2011, pp. 6785–6788.
[52] H. M. Power and R. J. Simpson, *Introduction to Dynamics and Control*. New York, NY, USA: McGraw-Hill, 1978.
[53] S. Marceglia, G. Foffani, A. M. Bianchi, G. Baselli, F. Tamma, M. Egidi, and A. Priori, "Dopamine-dependent non-linear correlation between subthalamic rhythms in Parkinson's disease," *J. Physiol.*, vol. 571, no. 3, pp. 579–591, 2006.
[54] S. Marceglia, A. Bianchi, G. Baselli, G. Foffani, F. Cogiamanian, N. Modugno, S. Mrakic-Sposta, A. Priori, and S. Cerutti, "Interaction between rhythms in the human basal ganglia: Application of bispectral analysis to local field potentials," *IEEE Trans. Neural Syst Rehabil. Eng.*, vol. 15, no. 4, pp. 483–492, Dec. 2007.
[55] A. Nambu, H. Tokuno, and M. Takada, "Functional significance of the cortico-subthalamo-pallidal "hyperdirect" pathway," *Neurosci. Res.*, vol. 43, no. 2, pp. 111–117, 2002.
[56] M. Rizzone, M. Lanotte, B. Bergamasco, A. Tavella, E. Torre, G. Faccani, A. Melcarne, and L. Lopiano, "Deep brain stimulation of the subthalamic nucleus in Parkinson's disease: Effects of variation in stimulation parameters," *J. Neurol., Neurosurg. Psychiatry*, vol. 71, no. 2, pp. 215–219, 2001.
[57] P. E. O'Suilleabhain, W. Frawley, C. Giller, and R. B. Dewey, "Tremor response to polarity, voltage, pulsewidth and frequency of thalamic stimulation," *Neurology*, vol. 60, no. 5, pp. 786–790, 2003.
[58] E. Moro, R. J. Esselink, J. Xie, M. Hommel, A. L. Benabid, and P. Pollak, "The impact on Parkinson's disease of electrical parameter settings in STN stimulation," *Neurology*, vol. 59, no. 5, pp. 706–713, 2002.

Authors' photographs and biographies are not available at the time of publication